Structural Engineering and Mechanics, *Vol. 47, No. 2 (2013) 185-207*
DOI: http://dx.doi.org/10.12989/sem.2013.47.2.185

Improving design limits of strength and ductility of NSC beam by considering strain gradient effect

J.C.M. Ho[*1] and J. Peng[2a]

[1]*School of Civil Engineering, The University of Queensland, QLD 4072, Australia*
[2]*Department of Civil Engineering, The University of Hong Kong, Hong Kong*

(Received November 10, 2011, Revised May 28, 2013, Accepted July 11, 2013)

Abstract. In flexural strength design of normal-strength concrete (NSC) beams, it is commonly accepted that the distribution of concrete stress within the compression zone can be reasonably represented by an equivalent rectangular stress block. The stress block is governed by two parameters, which are normally denoted by α and β to stipulate the width and depth of the stress block. Currently in most of the reinforced concrete (RC) design codes, α and β are usually taken as 0.85 and 0.80 respectively for NSC. Nonetheless, in an experimental study conducted earlier by the authors on NSC columns, it was found that α increases significantly with strain gradient, which means that larger concrete stress can be developed in flexure. Consequently, less tension steel will be required for a given design flexural strength, which improves the ductility performance. In this study, the authors' previously proposed strain-gradient-dependent concrete stress block will be adopted to produce a series of design charts showing the maximum design limits of flexural strength and ductility of singly- and doubly- NSC beams. Through the design charts, it can be verified that the consideration of strain gradient effect can improve significantly the flexural strength and ductility design limits of NSC beams.

Keywords: beams; concrete stress block; design; ductility; normal-strength concrete; strain gradient; strength

1. Introduction

It is generally accepted that the flexural strength evaluation of reinforced concrete (RC) beams can be achieved by replacing the nonlinear concrete stress distribution in compression zone with an equivalent rectangular stress block (Ibrahim and Macgregor 1996, Tan and Nguyen 2004). Fig. 1 shows the actual nonlinear concrete stress distribution and the respective equivalent rectangular stress block in the compression zone with parameters α and β. The method of using an equivalent rectangular stress block for concrete in compression has been commonly adopted in many of the current RC design codes (Standards Australia 2001, ECS 2004, NZS 2006, ACI 2008). In these codes, α and β are taken as 0.85 and 0.85 (0.80 for ECS) respectively, which are constant. The value of α = 0.85 is actually the ratio of the ultimate strength of NSC columns tested under concentric axial load to their respective concrete cylinder strength (Mattock *et al*. 1961, Ibrahim and MacGregor 1997). Table 1 summarises the values of α and β adopted by some RC design codes.

∗Corresponding author, Senior Lecturer, E-mail: johnny.ho@uq.edu.au
[a]Ph.D. Student

http://www.techno-press.org/?journal=sem&subpage=8 ISSN: 1225-4568 (Print), 1598-6217 (Online)

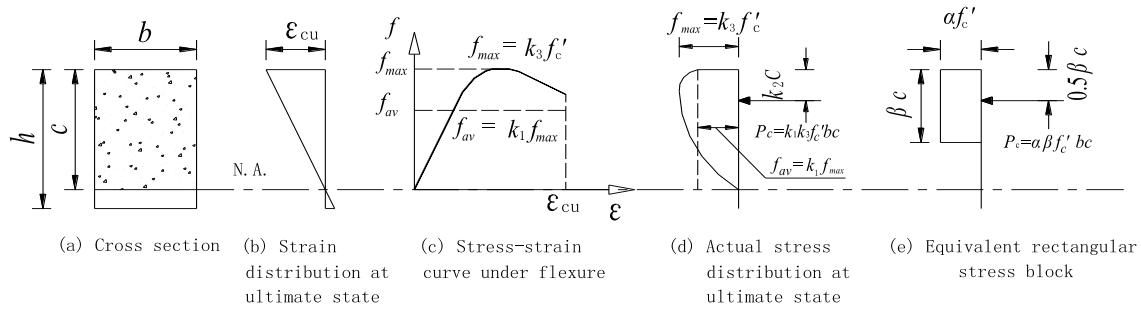

Fig. 1 Actual concrete stress distribution and its equivalent rectangular stress block

Table 1 Design values of equivalent concrete stress block parameters in codes

Design code	α	β
CI 318 (2008)	0.85 (for all f_c')	0.85 for $f_c' \le 28$Mpa $0.85 - 0.007(f_c'-28) \ge 0.65$ for $f_c' > 28$MPa
Eurocode 2 (2004)	0.85 for $f_c' \le 50$MPa $0.85-0.85\left(\frac{f_c'-50}{200}\right)$ for $50 < f_c' \le 90$MPa	0.80 for $f_c' \le 50$MPa $0.8-\left(\frac{f_c'-50}{400}\right)$ for $50 < f_c' \le 90$MPa
NZS3101 (2006)	0.85 for $0 < f_c' \le 55$MPa $0.85-0.004\left(f_c'-55\right)$ for $55 < f_c' \le 80$MPa 0.75 for $f_c' > 80$MPa	0.85 for $0 < f_c' \le 30$MPa $0.85-0.008\left(f_c'-30\right)$ for $30 < f_c' \le 55$MPa 0.65 for $f_c' > 55$MPa

By using the code specified values of α and β, a simple study has been conducted to compare the theoretical flexural strengths calculated using the codes with the experimentally measured strength M_t obtained by different researchers (Sheikh and Yeh 1990, Pecce and Fabrocino 1999, Mo and Wang 2000, Debernardi and Taliano 2002, Lam *et al*. 2003, Marefat *et al*. 2005). The comparison is summarized in Table 2. From the table, it is evident that: (1) The theoretical strengths are very close to the measured strength for columns subjected to $P/A_g f_c' > 0.5$ (axial load to axial capacity ratio > 0.5), in which difference is less than 5%. (2) The difference between the theoretical and measured flexural strengths is about 10% for NSC beams ($P/A_g f_c' = 0$). (3) The differences are about 19% and 23% for columns subjected to low and medium axial load levels. The above observations reveal that the specified value of $\alpha = 0.85$ in various RC codes could only predict accurately the flexural strength of NSC columns subjected to high and ultra-high axial load levels, but is too conservative for NSC beams and columns subjected to low or medium axial load level (i.e., $P/A_g f_c' \le 0.5$). Since the flexural strength underestimation is different for beams and columns, which are subjected to different strain gradient (defined as the ratio of ultimate concrete strain to neutral axis depth), it is believed that the value of α as well as the concrete stress developed in flexure, should also depend on the strain gradient. In the event that $\alpha = 0.85$, which was obtained from testing NSC columns under pure axial load without strain gradients (Hognestad *et al.* 1955, Mattock *et al.* 1961), is adopted for flexural strength calculation, it will underestimate the equivalent stress and hence flexural strength of the members.

The flexural strength underestimation of RC beam design should be treated with caution because it will underestimate the shear demand of the members (Pam and Ho 2001, Barchi *et al*. 2010) and

Table 2 Flexural capacity comparisons based on codes and experimental tests

Specimen code	f_c' (MPa)	$P/A_g f_c'$	M_{ACI} (kNm) (1)	M_{EC} (kNm) (2)	M_{NZ} (kNm) (3)	M_t (kNm) (4)	(1)/(4)	(2)/(4)	(3)/(4)
Beams									
A[a]	41.3	---	97.0	97.0	97.0	104.0	0.93	0.93	0.93
B[a]	41.3	---	45.0	45.0	45.0	49.6	0.91	0.91	0.91
T3[b]	27.7	---	28.9	29.3	28.9	32.5	0.89	0.90	0.89
T6[b]	27.7	---	170.5	171.2	170.5	192.4	0.89	0.89	0.89
Columns subjected to low axial load level									
C1-1[c]	24.9	0.113	300.5	305.1	300.5	351.4	0.86	0.87	0.86
C1-2[c]	26.7	0.106	303.8	308.2	303.8	374.6	0.81	0.82	0.81
C2-2[c]	27.1	0.156	325.2	330.5	325.2	399.9	0.81	0.83	0.81
Columns subjected to medium axial load level									
C3-3[c]	26.9	0.209	335.4	345.9	335.4	423.8	0.79	0.82	0.79
X6[d]	31.9	0.450	28.5	29.0	28.6	37.1	0.77	0.78	0.77
X7[d]	35.7	0.450	29.7	30.5	29.8	37.1	0.80	0.82	0.80
SBCM-8[e]	28.0	0.220	46.0	46.0	46.0	58.7	0.78	0.78	0.78
Columns subjected to high axial load level									
A-16[f]	33.9	0.600	157.1	159.1	157.6	157.5	1.00	1.01	1.00
E-2[f]	31.4	0.610	160.1	163.5	160.5	169.3	0.95	0.97	0.95
Columns subjected to ultra-high axial load level									
E-8[f]	25.9	0.780	128.4	129.2	128.4	129.2	0.99	1.00	0.99
E-10[f]	26.3	0.770	130.6	131.3	130.6	132.7	0.98	0.99	0.98

Notes:
[a]Pecce and Fabbrocino (1999); [b]Debernardi and Taliano (2002); [c]Mo and Wang (2000); [d]Lam *et al*. (2003); [e]Marefat *et al*. (2005); [f]Sheikh and Yeh (1990)

resistant RC structural members are provided with large amount of confining reinforcement (Pam and Ho 2009, Yan and Au 2010, Havaei and Keramati 2011, Ho 2011) or externally bonded steel plate (Su *et al*. 2009, Zhu and Su 2010) within the designed locations of plastic hinge regions based on beam-sideway collapse mechanism. To ensure such a mechanism can occur in reality, the flexural strength estimation of beams and columns should be accurate such that the designed locations of plastic hinge can actually form when subjected to large earthquake force or blasting (Weerheijm *et al*. 2009, Yagob *et al*. 2009).

Nonetheless, as seen from Table 2, the accuracies of flexural strength prediction as per existing RC codes are different for NSC beams and columns. Consequently, depending on the design axial load level of the columns, the predicted collapse mechanism may not be formed (Inel *et al*. 2008, Bechtoula *et al*. 2009, Sadjadi and Kianoush 2010). For example, if the design axial load level in columns is high, the actual beam strength will be larger than that of the columns and hence plastic hinge will form in the columns rather than in beams. This will change the collapse mechanism into a column-sideway mechanism, which is undesirable. Therefore, strain gradient effect should be taken into account to predict more accurately the locations of plastic hinges, deformability (Wu *et al*. 2004, Ho *et al*. 2010, Ho and Pam 2010) of members.

A lot of experimental research has already been conducted on the derivation of equivalent rectangular stress block for NSC (Hognestad *et al*. 1955, Mattock *et al*. 1961) and high-strength concrete (Attard and Setunge 1996, Ibrahim and MacGregor 1996, 1997, Attard and Stewart 1998,

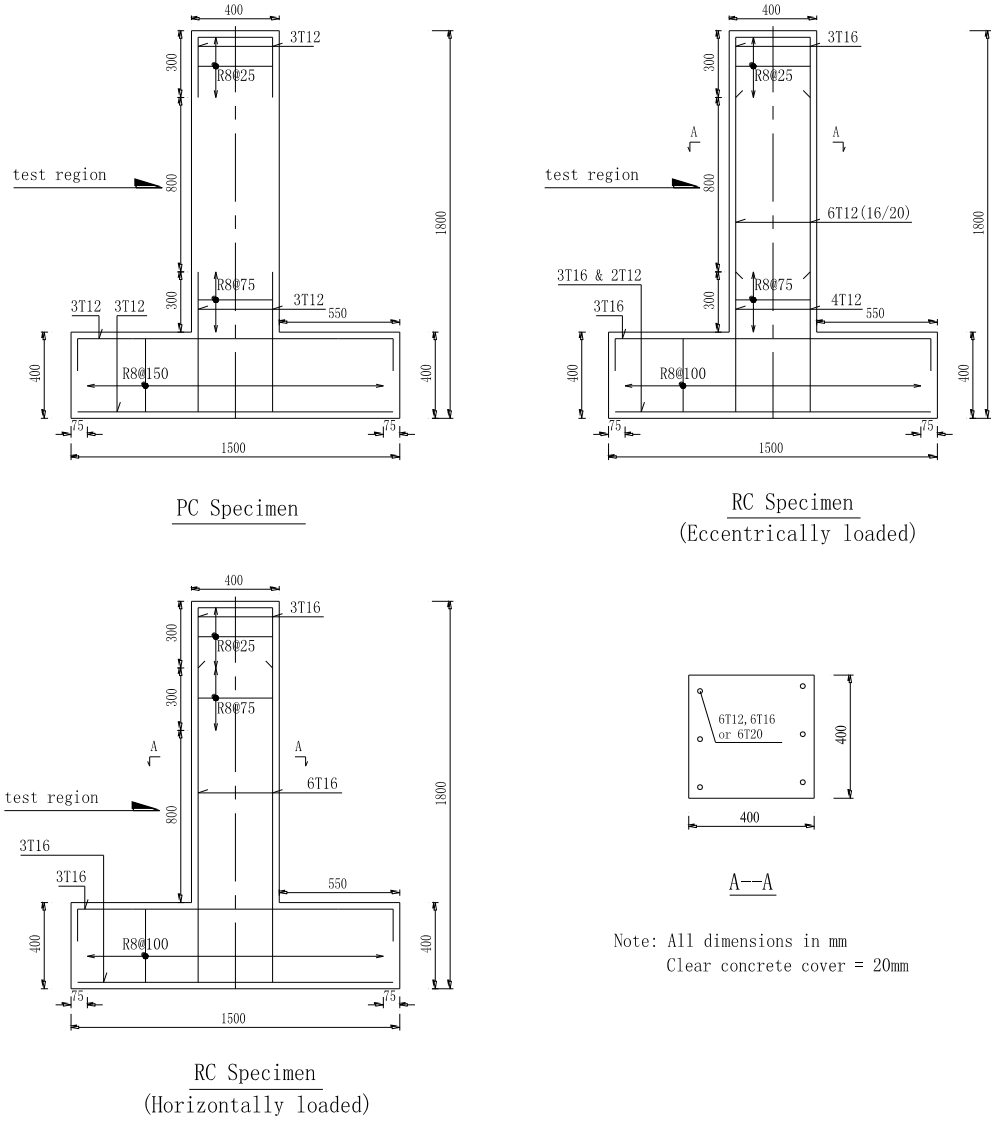

Fig. 2 Details of specimens and steel reinforcement

Ozbakkaloglu and Saatcioglu 2004, Tan and Nguyen 2004, 2005). From the results obtained for NSC columns, α is about 0.85 and depends only on the concrete strength. Therefore, for a given design requirement of flexural strength, the tension steel is more than it is needed because of the strength underestimation by the code. The results are that for a prescribed design flexural strength requirement, ductility decreases as more tension steel is required. In other words, the design limits of both flexural strength and ductility of NSC beams is reduced.

Recently, the authors have conducted an experimental study on the effect of strain gradient on the maximum concrete compressive stress that can be developed under flexure in NSC columns (Ho and

Table 3 Specimen property details

Group	Specimen code	Loading mode	Longitudinal steel				f_c' (MPa)		Eccentricity (mm)
			ρ_s (%)	Detail	f_y (MPa)	E_s (GPa)	28th day	Testing day	
1	PC30-0-CON	Concentric	0	---	---	---	29.6	30.0	0
	PC30-0-ECC	Eccentric	0	---	---	---		29.3	120
2	RC22-0.42-CON	Concentric	0.42	6T12	538	203	22.2	28.7	0
	RC22-0.42-ECC	Eccentric						28.7	140
3	RC22-0.75-CON	Concentric	0.75	6T16	533	203	21.9	27.4	0
	RC22-0.75-ECC	Eccentric						26.8	140
4	RC31-1.18-CON	Concentric	1.18	6T20	536	200	30.7	34.5	0
	RC31-1.18-ECC	Eccentric						34.3	110
5	RC46-0.75-CON	Concentric	0.75	6T16	515	203	45.6	45.6	0
	RC46-0.75-ECC-1	Eccentric						48.6	120
	RC46-0.75-ECC-2	Eccentric						48.6	140
6	RC34-0.75-CON	Concentric	0.75	6T16	498	198	33.6	35.2	0
	RC34-0.75-ECC-1	Eccentric						44.7	50
	RC34-0.75-ECC-2	Eccentric						44.7	130
	RC34-0.75-HOR-1	Horizontal load						35.2	---
	RC34-0.75-HOR-2	Horizontal load						35.2	---
7	RC51-0.75-CON	Concentric	0.75	6T16	517	192	51.0	54.8	0
	RC51-0.75-ECC-1	Eccentric						54.8	50
	RC51-0.75-ECC-2	Eccentric						54.8	140
	RC51-0.75-HOR-1	Horizontal						53.3	---
	RC51-0.75-HOR-2	Horizontal						53.3	---
8	RC41-0.75-CON	Concentric	0.75	6T16	529	202	41.0	41.0	0
	RC41-0.75-ECC-1	Eccentric						43.7	100
	RC41-0.75-ECC-2	Eccentric						41.9	140
	RC41-0.75-HOR	Horizontal						41.0	---

Peng 2011, Ho *et al*. 2011). From the test results, it was found that the relationship between α and strain gradient can be represented by a tri-linear curve. As a continued study, this paper will utilise the previously proposed values of α and β to investigate the flexural performance of NSC beams in terms of the limits of flexural strength and ductility that can be designed simultaneously. A set of design charts will be produced showing the design limits of NSC beams with strain gradient effect considered. It will be verified from the charts that the design limit of NSC beams can be improved significantly after the strain gradient effects has been considered.

2. Experimental programme

2.1 Details of test specimens

In a previous study conducted by the authors, a total of 25 inverted T-shape square column specimens (in 8 different groups) with concrete cylinder strength from 27 to 55 MPa and

longitudinal steel characteristic yield strength of 460 MPa and actual strength of above 500 MPa (Peng 2012) were fabricated and tested under concentric and eccentric axial loads as well as horizontal loads. The specimens within each group were of identical cross-section properties and materials' strength. The concrete within the same group of specimens can be reasonably regarded as having the same strength. In each group, one specimen was tested under concentric load (zero strain gradient), while the rest of them were tested under eccentric axial load (small strain gradient) or horizontal load (large strain gradient). The cross section of the specimens is 400×400 mm^2. The height of columns is 1400 mm and the length of supporting beams is 1500 mm, which are shown in Fig. 2. The plain concrete (PC) specimens did not contain any longitudinal steel within the testing region, while the RC specimens contained different amount of longitudinal steel (area ratio 0.42 – 1.18%) as shown in Table 3. The first number of the naming code of each of the specimens refers to the concrete cylinder strength on the 28^{th} day and the second number refers to the longitudinal steel ratio in percentage.

The uni-axial stress-strain behaviour of concrete in each group is taken as that of the concentrically loaded specimen. In all specimens, the concrete stress was obtained by subtracting the steel force (if any) from the total applied load and then the difference divided by the concrete area. The strain was obtained by dividing the average axial shortening of specimen measured by the LVDTs by its gauge length. On the other hand, the concrete stress-strain curve developed in flexure was obtained by modifying the concrete stress-strain curve obtained from the concentrically loaded specimens, such that theoretical axial load and moment match with the obtained experimental values. To investigate the effects of different extent of strain gradient, the loading eccentricities in columns varied from 50 to 140 mm as summarised in Table 3. The test setup for these three types of specimens is shown in Fig. 3.

(a) Specimen subjected to concentric load

(b) Specimen subjected to eccentric load

(c) Specimen subjected to horizontal and axial loads

Fig. 3 Testing scheme

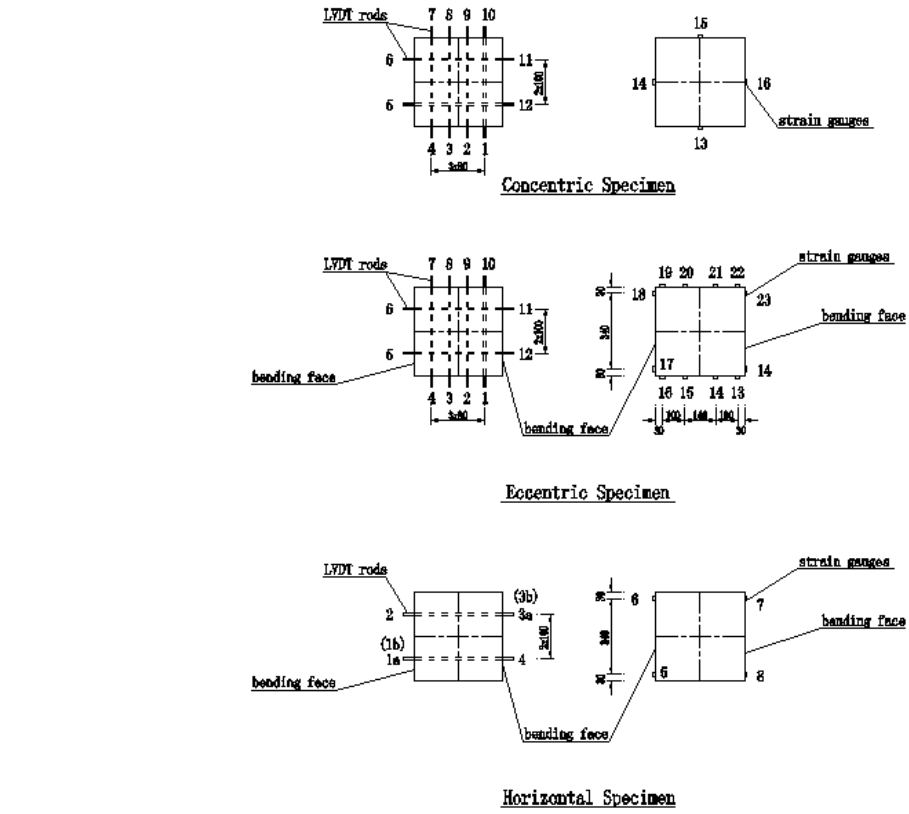

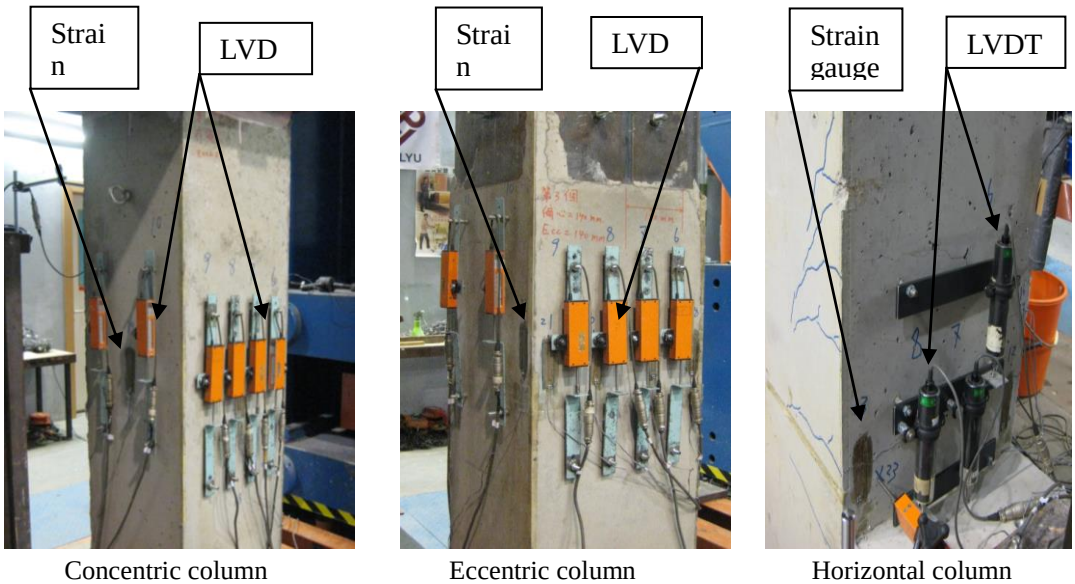

Concentric column Eccentric column Horizontal column

Fig. 4 Concrete strain gauges and LVDT instrumentations

2.2 Instrumentation

The following types of instrumentation were adopted:

(a) Strain gauges − Strain gauges for both steel and concrete were adopted. The steel strain gauges were attached to longitudinal steel bars located within the testing region. Also, concrete strain gauge(s) was/were attached on each face of every concentric and eccentric specimen. The details of strain gauges installation are shown in Fig. 4.

(b) Linear variable differential transducer (LVDT) − For each specimen, a total of 12 LVDTs were installed on four sides of the specimen within the test area to measure the deformation due to axial load and/or bending moment. The complete installation of LVDTs is also shown in Fig. 4.

2.3 Test procedure

For specimens subjected to concentric load, a 20 mm steel plate was installed on top of the column to ensure a smooth contact surface for loading application. For specimens subjected to eccentric load, a guided steel roller was installed at prescribed eccentricity on top of the aforementioned steel plate. In all specimens, the loading was applied in a displacement-controlled manner with a rate of 0.36 mm/min for concentric or eccentric specimens and 0.5 mm/min for horizontal specimens. All the data from the above instrumentation were recorded by a data logger. The loading process would stop after the applied load had reached the maximum value and then dropped below 80% of the maximum value.

3. Test results and interpretation

3.1 Test results of concentrically loaded specimens

Fig. 5(a) shows the failure condition of a specimen subjected to concentric load. The load-displacement and the evaluated stress-strain curves of concrete are shown in Fig. 6. It should be noted that the contribution of steel reinforcement in RC specimens is excluded in deriving the primary *y*-axis of the above graphs. The secondary *y*-axis, i.e., the concrete stress, is calculated by dividing the primary *y*-axis by the net concrete cross section area. The primary *x*-axis represents the average axial shortening measured by the LVDTs installed within the testing region. The secondary *x*-axis of strain is calculated by dividing the above measured average axial shortening by the gauge length of the LVDTs. The stress-strain curve in Fig. 6 will be adopted as the uni-axial stress-strain curve of concrete of all specimens within the same group.

3.2 Test results of eccentrically/horizontally loaded specimens

Figs. 5(b) and (c) show the failure condition of column specimens subjected to eccentric load and horizontal load respectively. The concrete compressive forces measured in the same way for the eccentrically loaded specimens are plotted against their respective measured vertical displacements in Fig. 7(a). Fig. 7(b) shows the graph of measured horizontal load plotted against the lateral drift of horizontally loaded columns. The moment acting on the eccentrically loaded specimens during test was evaluated by multiplying the applied axial load with the prescribed eccentricity because the columns were all relatively short (with slenderness ratio of 3.5) and the secondary moment due to

(a) Concentric column failure (b) Eccentric column failure (c) Horizontal column failure

Fig. 5 Failure conditions of specimens

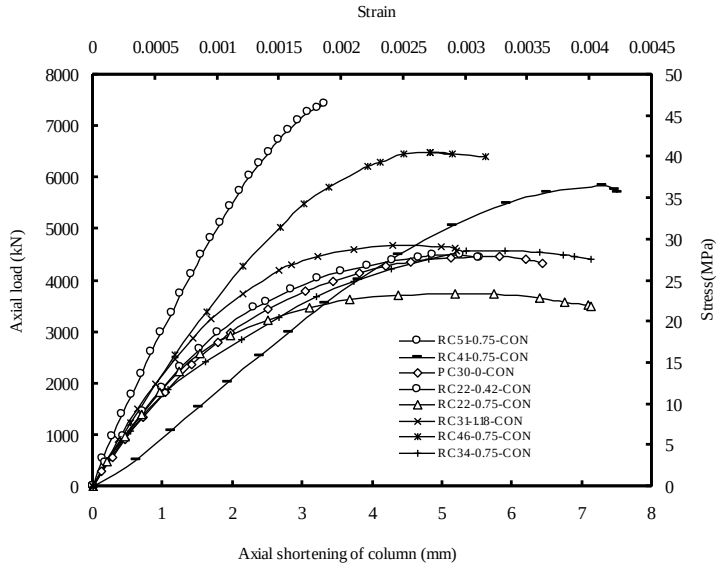

Fig. 6 Axial load-shortening and axial stress-strain curve of concentric specimens

column deflection was fairly negligible. For the horizontally loaded specimens, the moment was evaluated by multiplying the horizontal load with the vertical distance from the actuator to the beam-column interface.

4. Derivation of equivalent rectangular stress block

4.1 Derivation of stress-block parameters α and β

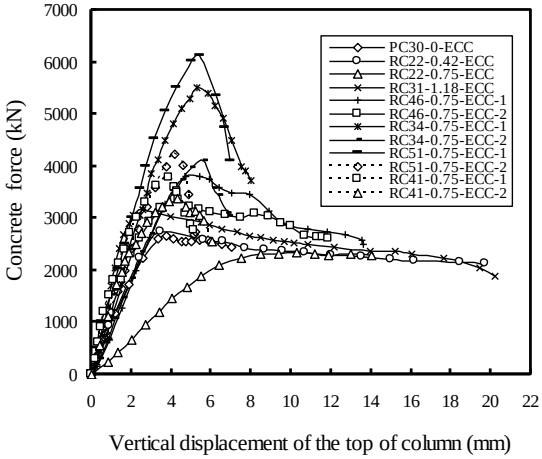

(a) Concrete compressive force against vertical displacement for eccentric specimens

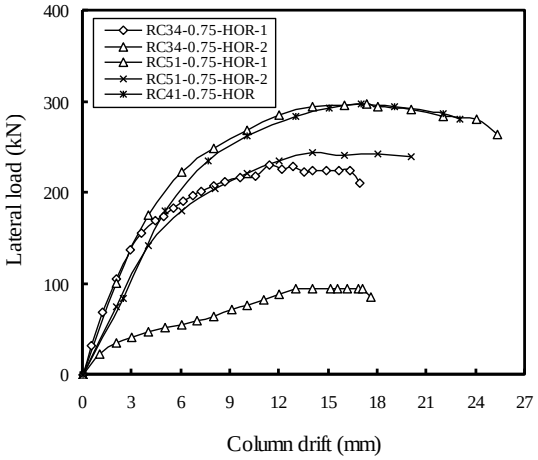

(b) Horizontal load against column drift for horizontal specimens

Fig. 7 Concrete force-vertical displacement and horizontal load-column drift curves of concrete of eccentrically and horizontally loaded specimens

In this section, the evaluation of equivalent rectangular concrete stress block parameter(s), i.e., α and/or β, for the concentrically, eccentrically and horizontally loaded specimens will be explained. The derivation of α and/or β is based on the axial load and/or moment equilibriums. For the concentrically loaded specimens, the value of α is determined from the axial force equilibrium condition as shown in Eq. (1a):

Axial force

$$P_e = \alpha\, f_c' b h + \sum_{i=1}^{n} f_{si}\, A_{si} \tag{1a}$$

where P_e is measured axial load of concentrically loaded specimens in the experiment and the expression on the right-hand side represents the theoretical axial load calculated using Fig. 1(e). For

the eccentrically and horizontally loaded specimens, the values of α and β are derived based on both axial force and moment equilibrium conditions to match the theoretical axial load and moment calculated using the equivalent rectangular stress block as shown in Fig. 1(e) with the respective measured values in the experiment. The equilibrium equations are expressed as follows:
Axial force

$$P_e = \alpha \beta f_c' b c + \sum_{i=1}^{n} f_{si} A_{si} \tag{1b}$$

Moment

$$M_e = \alpha \beta f_c' b c \left(\frac{h}{2} - \frac{\beta}{2} c \right) + \sum_{i=1}^{n} f_{si} A_{si} \left(\frac{h}{2} - d_i \right) \tag{1c}$$

where M_e is the measured moment of eccentrically or horizontally loaded specimen and the expressions on the right-hand side represent the theoretical axial load and moment calculated by Fig. 1(e).

The neutral axis depth c in the above equations is evaluated based on the modified concrete stress-strain curve obtained from the concentrically loaded specimens.

$$P_e = \int_{A_c} k_3 \sigma_c(\varepsilon) dA_c + \sum_{i=1}^{n} f_{si} A_{si} \tag{2a}$$

$$M_e = \int_{A_c} k_3 \sigma_c(\varepsilon) \left(\frac{h}{2} - c + x \right) dA_c + \sum_{i=1}^{n} f_{si} A_{si} \left(\frac{h}{2} - d_i \right) \tag{2b}$$

$$\varepsilon = \frac{x}{c} \varepsilon_{cu} \tag{2c}$$

where $\sigma_c(\varepsilon)$ is the concrete stress-strain curve obtained from the concentrically loaded specimens. It is assumed that the concrete stress-strain curve subjected to concentric load varies in a parabolic manner which can be described by a second-order polynomial. The details of the parabolic concrete stress-strain curve have been described and explained in earlier in Peng *et al*. (2012). k_3 is ratio of the maximum concrete stress developed under flexure to that in uni-axial condition; ε is the strain in concrete; A_c is the area of concrete compression zone, x is the distance of strip dA_c from the neutral axis; n is the total number of steel bars, f_{si} and A_{si} are respectively the stress and area of the i^{th} steel bar, d_i is the distance of the i^{th} steel bar from the extreme concrete compressive fibre, ε_{cu} is the ultimate concrete strain.

The values of α and β are summarised in Table 4. The values of α for the concentrically loaded specimens are also listed in the same table. From the table, it is clear that: (1) The value of α for the eccentrically/horizontally loaded specimens subjected to strain gradient is larger than that of the corresponding concentrically loaded specimens. Therefore, the strain gradient would have beneficial effect on the equivalent concrete stress developed in flexural RC members. (2) The value of α for the eccentrically/horizontally loaded specimens increases as the strain gradient increases until reaching a maximum value. (3) The average value of α obtained for the concentrically loaded columns is about 0.853, which is very close to the current design value of α = 0.85 stipulated in

Table 4 Equivalent rectangular concrete stress block parameters obtained in tests

Specimen code	α	β	ε_{cu}	ϕ (rad/m)	d/c
PC30-0-CON	0.937	---	0.0036	0.0	0.0*
RC22-0.42-CON	0.819	---	0.0031	0.0	0.0
RC22-0.75-CON	0.858	---	0.0033	0.0	0.0
RC31-1.18-CON	0.849	---	0.0029	0.0	0.0
RC46-0.75-CON	0.840	---	0.0029	0.0	0.0
RC-34-0.75-CON	0.815	---	0.0034	0.0	0.0
RC51-0.75-CON	0.850	---	0.0024	0.0	0.0
RC41-0.75-CON	0.805	---	0.0030	0.0	0.0
Average	0.853	---	0.0031	0.0	0.0
PC30-0-ECC	1.426	0.802	0.0036	0.0176	2.01*
RC22-0.42-ECC	1.323	0.806	0.0031	0.0142	1.721
RC22-0.75-ECC	1.357	0.783	0.0036	0.0135	1.622
RC31-1.18-ECC	0.898	0.794	0.003	0.0101	1.287
RC46-0.75-ECC-1	0.962	0.785	0.0031	0.0139	1.444
RC46-0.75-ECC-2	0.986	0.765	0.0031	0.0135	1.632
RC34-0.75-ECC-1	0.881	0.763	0.0035	0.0081	0.897
RC34-0.75-ECC-2	1.177	0.759	0.0034	0.0141	1.556
RC34-0.75-HOR-1	1.449	0.768	0.0036	0.0434	4.789
RC34-0.75-HOR-2	1.513	0.753	0.0036	0.1148	13.481
RC51-0.75-ECC-1	0.856	0.738	0.0035	0.0082	0.873
RC51-0.75-ECC-2	1.206	0.723	0.0029	0.0133	1.670
RC51-0.75-HOR-1	1.436	0.720	0.0030	0.045	5.515
RC51-0.75-HOR-2	1.455	0.726	0.0031	0.066	7.744
RC41-0.75-ECC-1	0.845	0.821	0.0031	0.011	1.291
RC41-0.75-ECC-2	1.100	0.778	0.0032	0.015	1.655
RC41-0.75-HOR	1.387	0.785	0.0034	0.027	2.844
Average	---	0.770	0.0033	---	---

various RC design codes (ACI 2008, Standards Australia 2001, ECS 2004, Standards New Zealand 2006). (4) The values of β are insensitive to the extent of strain gradient.

4.2 Tri-linear equation for α

It can be easily observed from Table 4 that the value α depends significantly on strain gradient, which increases as strain gradient increases. This implies that the concrete compressive stress is enhanced due to strain gradient effect in flexural members. On the other hand, the value of β remains relatively constant with strain gradient, which implies that the resultant of concrete compression is insensitive to the strain gradient developed in flexural members. The variations of α and β with strain gradient ϕ are correlated using regression analysis from the results obtained. However, since ϕ is a non-dimensionless factor, its adoption in the correlation will include the effect of column size. Therefore, it is proposed in this study to use a dimensionless parameter to eliminate the size effect, which is the ratio of effective depth to neutral axis depth, i.e., d/c.

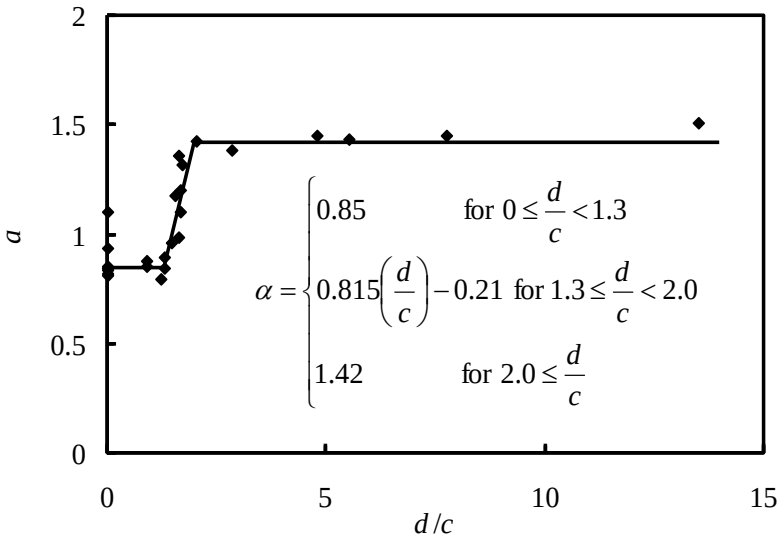

(a) α plotted against d/c

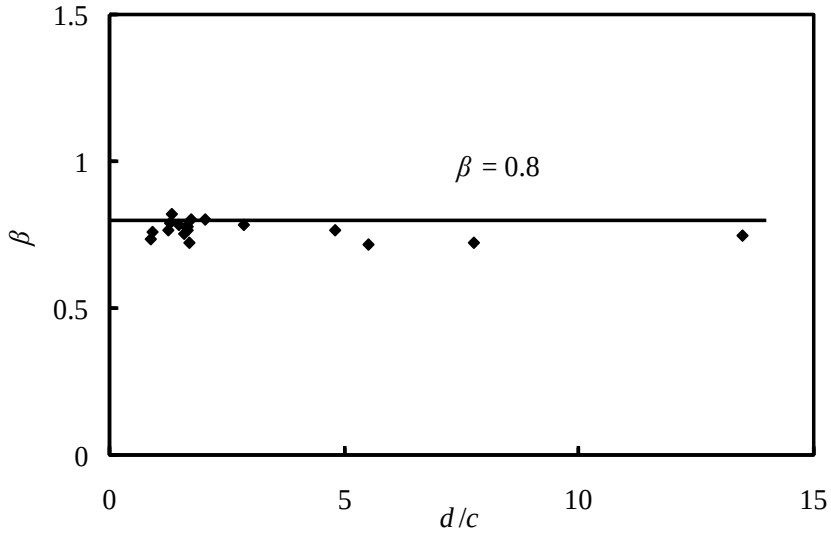

(b) β plotted against d/c

Fig. 8 α and β plotted against strain gradient d/c

The values of α and β obtained from the eccentrically and horizontally loaded specimens are plotted against d/c in Figs. 8(a) and 8(b). From Fig. 8(a), it is apparent that the change rate of α with respect to d/c is not constant and dependent on the value of d/c. A tri-linear curve is proposed to correlate the variation of α with d/c. To summarise, the variation of α with d/c is represented by the following tri-linear curve

$$\alpha = \begin{cases} 0.85 & \text{for } 0 \le \dfrac{d}{c} < 1.3 \\ 0.815\left(\dfrac{d}{c}\right) - 0.21 & \text{for } 1.3 \le \dfrac{d}{c} < 2.0 \\ 1.42 & \text{for } 2.0 \le \dfrac{d}{c} \end{cases} \tag{3a}$$

On the contrary, it is seen from Fig. 8(b) that the value of β remains fairly constant at $\beta = 0.8$, which is insensitive to the strain gradient. Hence

$$\beta = 0.80 \tag{3b}$$

4.3 Ultimate concrete strain ε_{cu}

From Table 4, it is evident that the values of ultimate concrete strain ε_{cu} for various eccentrically/horizontally loaded specimens vary within a narrow range from 0.0029 to 0.0036. For practical design purpose in evaluating the flexural strength of NSC members based on the previously proposed equivalent rectangular concrete stress block, it is proposed to use the fixed value of ε_{cu} = 0.0033, which is the average value of the obtained ε_{cu}.

4.3 Verification against experimental results

To validate the obtained equivalent rectangular concrete stress block parameters, the proposed value of α and β given respectively in Eqs. (3a) and (3b), as well as the proposed value of ε_{cu} = 0.0033 are used to evaluate the flexural strengths of RC beams tested by other researchers (Pecce and Fabbrocino 1999, Ashour 2000, Pam *et al*. 2001a, Debernardi and Taliano 2002, Lam *et al*. 2008, Fathifazl *et al*. 2009). These predicted flexural strengths M_p are compared with their respective measured strengths M_t as well as with their respective theoretical strengths based on various RC design codes, i.e., M_{ACI} based on ACI Code, M_{EC} based on Eurocode 2 and M_{NZ} based on New Zealand Code. The comparison is summarised in Table 5.

From Table 5, it can be concluded that:

(1) The flexural strengths of RC beams predicted by the proposed values of α, β and ε_{cu} have the best agreement with their measured flexural strengths.

(2) The average ratio of the predicted to measured flexural strength is 0.96, whereas the respective ratios of the theoretical to measured flexural strength of ACI, EC2 and NZS are 0.89, 0.90 and 0.89. It is evident that the proposed method can increase the accuracy of flexural strength prediction by 7% in average.

(3) It is observed that the accuracy of flexural strength predicted by using the proposed values of α, β and ε_{cu} improves for RC beams. This indicates that the proposed equivalent rectangular concrete stress block, which depends on strain gradient, represents more accurately the equivalent concrete stress developed under flexure.

5. Improving design limits of flexural strength and ductility of NSC beams

Table 5 Flexural strength prediction comparisons of beams

Specimen code	f_c'	M_p (1)	M_{ACI} (2)	M_{EC} (3)	M_{NZ} (4)	M_t (5)	(1)/(5)	(2)/(5)	(3)/(5)	(4)/(5)
Pecce and Fabbrocino (1999)										
A	41.3	93.6	97.0	97.0	97.0	104.0	0.90	0.93	0.93	0.93
B	41.3	47.3	45.0	45.0	45.0	49.6	0.95	0.91	0.91	0.91
C	42.3	705.1	636.7	636.7	636.7	712.5	0.99	0.89	0.89	0.89
Ashour (2000)										
B-N2	48.6	64.3	53.6	53.6	53.6	58.2	1.10	0.92	0.92	0.92
B-N3	48.6	69.7	77.1	77.1	77.1	80.6	0.87	0.96	0.96	0.96
B-N4	48.6	104.6	98.4	98.4	98.4	99.6	1.05	0.99	0.99	0.99
Pam *et al*. (2001)										
1	29.9	54.5	56.1	56.1	56.1	77.6	0.70	0.72	0.72	0.72
2	29.4	83.0	80	80.0	80	103.5	0.80	0.77	0.77	0.77
3	29.1	122.7	114.1	111.5	114.1	126.5	0.97	0.90	0.88	0.90
4	33.8	122.1	112.0	112.7	112.0	129.0	0.95	0.87	0.87	0.87
5	37.1	137.6	133.8	134.8	133.8	142.8	0.96	0.94	0.94	0.94
6	34.6	166.5	144.8	139.6	144.8	162.0	1.03	0.89	0.86	0.89
7	46.9	151.2	145.7	162.3	145.7	164.6	0.92	0.89	0.89	0.89
8	45.7	168.9	160.6	161.4	160.6	166.2	1.02	0.97	0.97	0.97
Debernardi and Taliano (2002)										
T1	27.7	16.2	10.8	10.8	10.8	13.6	1.19	0.79	0.79	0.79
T2	27.7	25.0	20.5	20.6	20.5	23.6	1.06	0.87	0.87	0.87
T3	27.7	33.5	28.9	29.3	28.9	32.5	1.03	0.89	0.90	0.89
T4	27.7	53.4	46.9	46.8	46.9	59.8	0.89	0.78	0.78	0.78
T5	27.7	98.5	93.1	93.1	93.1	107.5	0.92	0.87	0.87	0.87
T6	27.7	182.3	170.5	171.2	170.5	192.4	0.95	0.89	0.89	0.89
T8	27.7	85.6	81.1	81.2	81.1	93.9	0.91	0.86	0.86	0.86
T9	27.7	158.8	152.0	151.9	152.0	182.7	0.87	0.83	0.83	0.83
Lam *et al*. (2008)										
L-C1	29.8	15.5	14.6	14.6	14.6	14.2	1.09	1.03	1.03	1.03
L-D	29.8	10.4	9.8	9.8	9.8	11.6	0.90	0.84	0.84	0.84
L-E	29.8	31.3	25.9	26.0	25.9	29.4	1.06	0.88	0.89	0.88
Fathifazl *et al*. (2009)										
EV-2.7N	43.5	105.5	108.3	108.4	108.3	126.4	0.83	0.86	0.86	0.86
CG-2.7N	43.5	110.7	106.3	106.3	106.3	118.5	0.93	0.90	0.90	0.90
Average							0.96	0.89	0.90	0.89

It is evident from the above test results that the maximum concrete stress developed in flexural RC members increases as strain gradient increases, the effect of which has been neglected in the current RC design codes because of conservative reason. This will lead to an underestimation of the flexural strength of NSC beams and columns. The major drawback of this is that it will lower the design limits of flexural strength and ductility of NSC beams since more tension steel is required for a given design strength requirement when strain gradient effect is neglected. Therefore in this study, the tri-linear relationship of concrete stress developed in flexure with strain gradient effect considered will be adopted to produce a set of strength-ductility diagrams (Ho *et al*. 2004). Different concrete strength will be used and the results will be compared with those obtained without strain

gradient considered. It will be shown later in this section that the maximum design limits in terms of flexural strength and ductility are improved significantly for NSC beams when strain gradient effect is considered.

5.1 Singly-reinforced NSC beams

The proposed equivalent rectangular stress block for NSC was applied to evaluate the flexural strength of singly-reinforced NSC beams with various tension steel contents and concrete strength. From Fig. 1(e), the flexural strength M of a singly-reinforced beam section can be evaluated using axial force and moment equilibriums:
Axial force equilibrium

$$\alpha\beta f_c' bc = f_{st}\rho_t bd \tag{4a}$$

Moment equilibrium

$$M = \alpha\beta f_c' bc(d - 0.5\beta c) \tag{4b}$$

where α and β are obtained from Eqs. (3a) and (3b) respectively, $\rho_t = A_{st}/bd$, A_{st} is the tension steel area, f_{st} is the stress in tension steel and b is the breadth of section. However, it should be noted that α depends on d/c, therefore the determination of neutral axis depth c and hence flexural strength M of the beam section is an iterative process.

For the evaluation of the flexural ductility of NSC beams, a previously established equation by the authors is adopted (Ho *et al*. 2003), which is rewritten as Eq. (5). It should be noted that the value of f_{co} is taken as $\alpha f_c'$, which is the concrete stress developed in flexure, rather than the uni-axial concrete cylinder strength f_c'.

$$\mu = 10.7\,(f_{co})^{-0.45}((\rho_t - \rho_c)/\rho_{bo})^{-1.25} \tag{5}$$

where ρ_c is the compression steel ratio (= 0 for singly-reinforced beams) and ρ_{bo} is the balanced steel ratio, the value of which can be obtained from Ho *et al*. (2003). The steel yield strength is set to 500 MPa.

The flexural strength and ductility results obtained from Eqs. (4) and (5) can be plotted in the form of graph, which also indicates the maximum design limits. The y-axis refers to the ductility while the x-axis is the normalised flexural strength $M/(bd^2)$. The respective strength-ductility graph for different concrete strength f_{co} = 30, 40 and 50 MPa have been plotted in Fig. 9(a). The curves in the figure show the maximum flexural strength and ductility that can be achieved by singly RC beams simultaneously. The corresponding tension steel ratio can be read from the intermediate lines. For a given design requirement of strength and ductility, the possible combination of concrete strength and tension steel ratio can be obtained rapidly from the graph, which enables both strength and ductility design of singly-reinforced NSC beams in just one step.

5.2 Doubly-reinforced NSC beams

If compression steel is added, other sets of chart corresponding to various compression steel ratios are needed. Based on the same principle, the proposed equivalent rectangular stress block for NSC with strain gradient effect considered could be applied to evaluate the flexural strength of

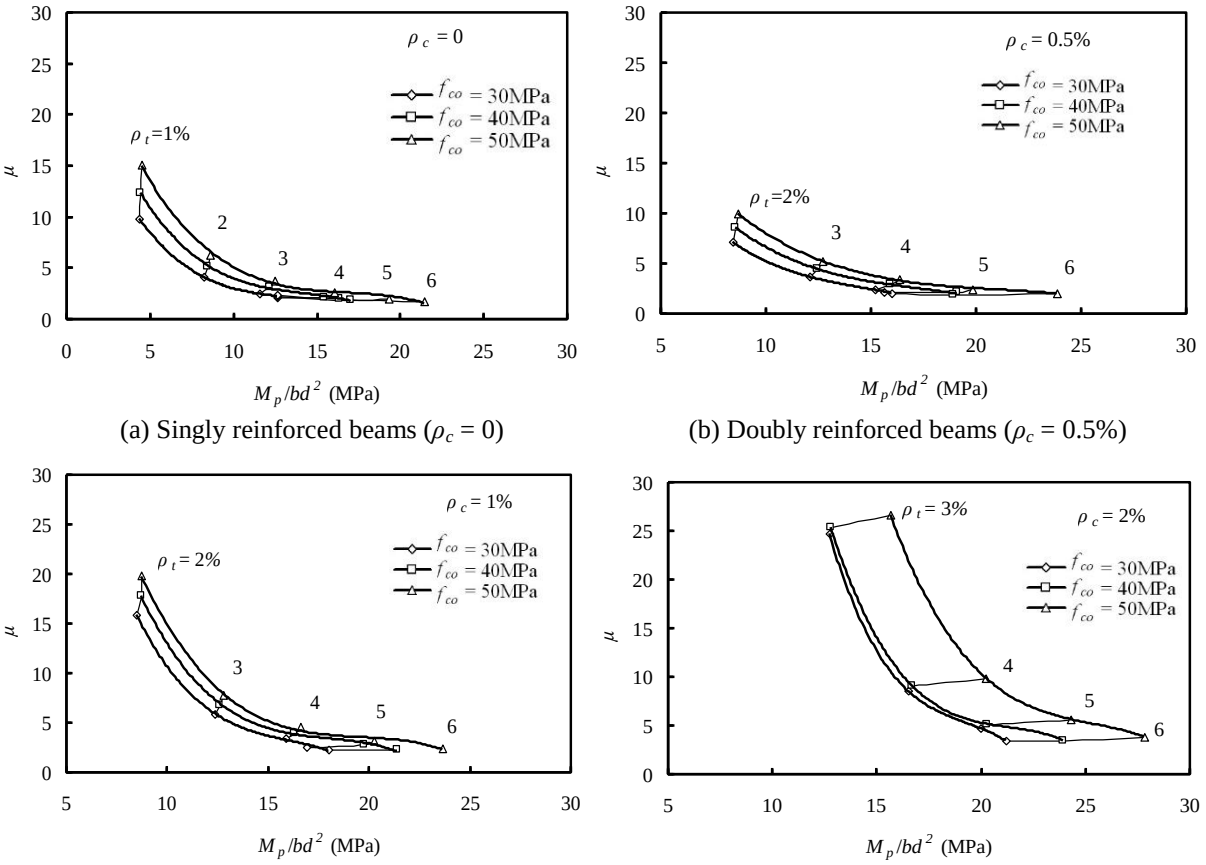

(a) Singly reinforced beams (ρ_c = 0) (b) Doubly reinforced beams (ρ_c = 0.5%)

(c) Doubly reinforced beams (ρ_c = 1%) (d) Doubly reinforced beams (ρ_c = 2%)

Fig. 9 Strength-ductility graphs for singly and doubly reinforced concrete beams

doubly-reinforced NSC beam sections using the following equations:
Axial force equilibrium

$$\alpha\beta f_c' bc + f_{sc}\rho_c bd = f_{st}\rho_t bd \tag{6a}$$

Moment equilibrium

$$M = \alpha\beta f_c' bc(d - 0.5\beta c) + f_{sc}\rho_c bd(d - d') \tag{6b}$$

where $\rho_c = A_{sc}/bd$, A_{sc} is the compression steel area, f_{sc} is the stress in compression steel, d' is the distance from the extreme compressive fibre to the centroid of compression steel. For practical design application, a series of design charts plotting the flexural strength in terms of $M/(bd^2)$ against flexural ductility for compression steel ratios of 0.5, 1.0 and 2.0% (practical range of compression steel ratio), tension steel ratios up to 6% and concrete strengths from 30 to 50 MPa are shown in Fig. 9(b) to 9(d). The value of d'/d adopted in Fig. 9 is equal to 0.12. The steel yield strength is set to 500 MPa.

For the evaluation of the flexural ductility of NSC beams, a previously established equation by

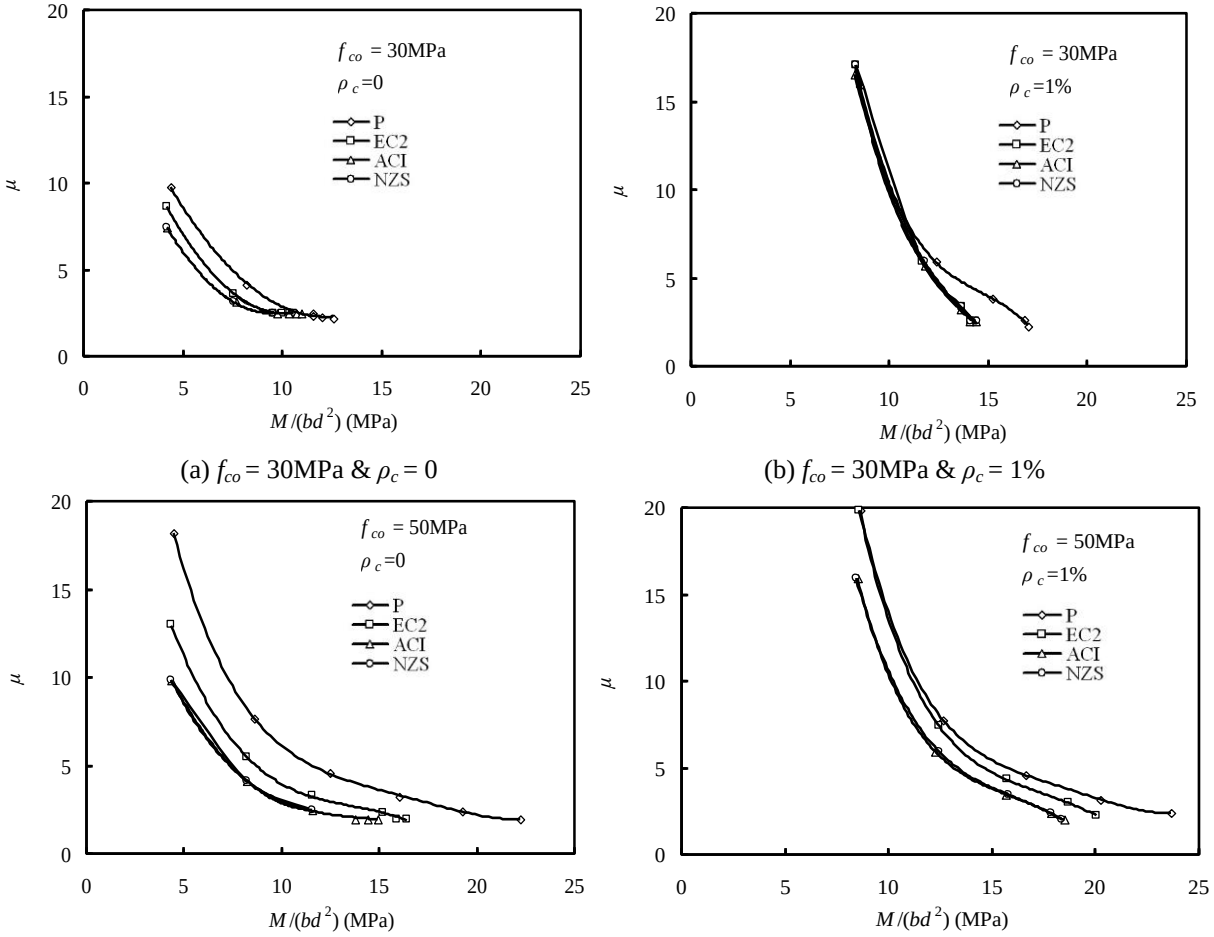

(a) f_{co} = 30MPa & ρ_c = 0 (b) f_{co} = 30MPa & ρ_c = 1%

(c) f_{co} = 50MPa & ρ_c = 0 (d) f_{co} = 50MPa & ρ_c = 1%

(Note: P denotes the proposed strength-ductility graph, while ACI, EC2 and NZS are those evaluated from current RC design codes)

Fig. 10 Strength-ductility graphs comparison

the authors is adopted (Pam *et al*. 2001b), which is rewritten as Eq. (7).

$$\mu = 10.7\,(f_{co})^{-0.45}((\rho_t - \rho_c)/\rho_{bo})^{-1.25}(1 + 95.2(f_{co})^{-1.1}(\rho_c/\rho_t)^3) \quad (7)$$

Each of the graphs above represents the design limit for a particular compression steel ratio for beam sections having f_{co} = 30-50 MPa. The corresponding tension steel ratio can be read from the intermediate lines. For a given design requirement of strength and ductility, the possible combination of concrete strength, tension and compression steel ratios can be obtained directly from these graphs, which enable both strength and ductility design of doubly-reinforced NSC beams in just one step.

5.3 Comparison with current RC design codes

As discussed before, because of a more accurate prediction of flexural strength of NSC beams when strain gradient effect is taken into account, the tension steel required for a given flexural strength design requirement is smaller. It in turns increases the ductility capacity for the same design flexural strength. Consequently, the maximum design limits of flexural strength and ductility that can be achieved simultaneously increase. The extent of improvement can be studied by plotting the same strength-ductility graphs using two different approaches, i.e. without strain gradient effect as per various current RC design codes (EC2 2004, NZS3101 2006, ACI 2008) and with strain gradient as per Eqs. (3), (5) and (7).

The evaluation has been carried out for the following beam sections with f_{co} = 30, 50 MPa and ρ_c = 0 and 1% using those two approaches. The obtained strength-ductility graphs are shown in Fig. 10. From the figures, it is evident that:

(1) The strength-ductility performance obtained as per various design codes is very similar, except for EC2 at 50 MPa, where there is a sudden change in α and β values. This is because the equivalent rectangular stress block parameters for NSC stipulated in these codes are very close to each other, which are strain-gradient independent, especially for lower concrete strength and doubly reinforced beams.

(2) The strength-ductility curves with strain gradient effect considered are located on the upper right-hand side of other curves without strain gradient effect considered, which means that there is improvement on strength-ductility performance, especially for singly reinforced beams.

(3) Given the same flexural strength design requirement (i.e., same *x*-value), the consideration of strain gradient effect can improve significantly the limit of ductility that the beams can achieve. Conversely, given the same ductility design requirement (i.e., same *y*-value), the consideration of strain gradient effect can improve significantly the limit of flexural strength the beams can achieve.

(4) In other words, the consideration of strain gradient effects can improve both limits of strength and ductility that can be designed (i.e. both *x*- and *y*-values increased) at the same time.

6. Conclusions

The equivalent rectangular concrete stresses that can represent the concrete compressive stress distribution in flexural NSC members was studied experimentally in this study. Eight groups of inverted T-shaped specimens were fabricated, each of which consists of specimens with identical cross-section properties. In each group, one of the specimens was subjected to concentric axial load while the rest were subjected to eccentric axial load or combined axial and lateral loads. To investigate the effect of strain gradient on the equivalent rectangular concrete stress block, the stress block parameters (α and β) that can be developed were evaluated by matching the theoretical and experimental axial loads and moments of the tested specimens.

From the obtained result, it was evident that the value of α, which is the ratio of the equivalent concrete stress to concrete cylinder strength, were significantly larger than the respective value stipulated in the current RC design codes (i.e., α = 0.85). It has also been verified in this study the α value stipulated represent only for the concrete stress developed in uni-axial stress state. More importantly, it was found that the value of α were dependent on strain gradient. An empirical formula has been proposed for the relation between α and strain gradient, the later of which was represented by a dimensionless factor *d*/*c* (i.e., ratio of effective to neutral axis depths) to eliminate size effect. A tri-linear curve was proposed for the variation of α with *d*/*c* for design purpose. On the

other hand, the value of β which is the ratio of the depth of the stress block to neutral axis depth remains relatively constant at 0.80.

The validity of the proposed equivalent rectangular stress block, which takes into account the effects of strain gradient, was checked by comparing the theoretical strength of beams with the their measured strength obtained by other researchers. Then, the proposed equivalent rectangular stress block was applied to investigate the improvement in the maximum design limits of flexural strength and ductility that can be achieved simultaneously in the NSC beams design. Design charts were produced for both singly- and doubly-reinforced NSC beams with different concrete strength, tension and compression steel ratios. By comparing the design limits of flexural strength and ductility for singly- and doubly-reinforced NSC beams with those predicted by various current RC design codes, it is seen that the strain gradient effect can improve significantly the flexural strength at constant ductility, or flexural ductility at constant strength, or both flexural strength and ductility simultaneously.

Acknowledgements

The research grant from Seed Funding Programme for Basic Research (account code 10401445) of The University of Hong Kong (HKU) for the work presented herein is gratefully acknowledged. The authors gratefully thank the Department of Civil and Structural Engineering, The Hong Kong Polytechnic University (PolyU), where most of the experimental tests were conducted. Also, supports from the technical staff in the structural laboratory of PolyU and the Department of Civil Engineering, HKU, are greatly appreciated.

References

ACI Committee 318 (2008), *Building Code Requirements for Reinforced Concrete and Commentary ACI 318M-08*, Manual of Concrete Practice, American Concrete Institute, Michigan, USA.

Ashour, S.A. (2000), "Effect of compressive strength and tensile reinforcement ratio on flexural behaviour of high-strength concrete beams", *Engineering Structures*, **25**(8), 1083-1096.

Attard, M.M. and Setunge, S. (1996), "The stress strain relationship of confined and unconfined concrete", *ACI Materials Journal*, **93**(5), 432-442.

Attard, M.M. and Stewart, M.G. (1998), "A two parameter stress block for high-strength concrete", *ACI Structural Journal*, **95**(3), 305-317.

Barchi, M., Azadbakht, M. and Hadad, M. (2010), "Evaluating the ductility and shear behaviour of carbon fibre reinforced polymer and glass fibre reinforced polymer reinforced concrete columns", *The Structural Design of Tall and Special Buildings*, **21**(4), 249-264.

Bechtoula, H., Kono, S. and Watanabe, F. (2009), "Seismic performance of high strength reinforced concrete columns", *Structural Engineering and Mechanics*, **31**(6), 697-716.

Debernardi, P.G. and Taliano, M. (2002), "On evaluation of rotation capacity for reinforced concrete beams", *ACI Structural Journal*, **99**(3), 360-368.

European Committee for Standardization (ECS) (2004), *Eurocode 2: Design of Concrete Structures: Part 1-1: General Rules and Rules for Buildings*, British Standard Institution, London, UK.

Fathifazl, G., Razaqpur, A.G., Isgor, O.B., Abbas, A., Fournier, B. and Foo, S. (2009), "Shear strength of reinforced recycled concrete beams without stirrups", *Magazine of Concrete Research*, **61**(7), 477-490.

Havaei, G.R. and Keramati, A. (2011), "Experimental and numerical evaluation of the strength and ductility of regular and cross spirally circular reinforced concrete columns for tall buildings under eccentric loading",

The Structural Design of Tall and Special Buildings, **20**(2), 247-256.
Ho, J.C.M., Kwan, A.K.H. and Pam, H.J. (2003), "Theoretical analysis of post-peak flexural behaviour of normal- and high-strength concrete beams", *The Structural Design of Tall and Special Buildings*, **12**(2), 109-125.
Ho, J.C.M., Kwan, A.K.H. and Pam, H.J. (2004), "Minimum flexural ductility design of high-strength concrete beams", *Magazine of Concrete Research*, **56**(1), 13-22.
Ho, J.C.M. (2011), "Limited ductility design of reinforced concrete columns for tall buildings in low to moderate seismicity regions", *The Structural Design of Tall and Special Buildings*, **20**(1), 102-120.
Ho, J.C.M., Lam, J.Y.K. and Kwan, A.K.H. (2010), "Flexural ductility and deformability of concrete beams incorporating high-performance materials", *The Structural Design of Tall and Special Buildings*, **21**(2), 114-132.
Ho, J.C.M. and Peng, J. (2011), "Strain gradient effects on flexural strength design of normal-strength concrete columns", *Engineering Structures*, **33**, 18-31.
Ho, J.C.M., Pam, H.J., Peng, J. and Wong, Y.L. (2011), "Maximum concrete stress for flexural RC members", *Computers and Concrete*, **8**(2), 207-227.
Ho, J.C.M. and Pam, H.J. (2010), "Deformability evaluation of high-strength reinforced concrete columns", *Magazine of Concrete Research*, **62**(8), 569-583.
Hognestad, E., Hanson, N.W. and McHenry, D. (1955), "Concrete stress distribution in ultimate strength design", *ACI Journal*, **52**(12), 455-480.
Ibrahim, H.H.H. and MacGregor, J.G. (1996), "Flexural behavior of laterally reinforced high-strength concrete sections", *ACI Structural Journal*, **93**(6), 674-684.
Ibrahim, H.H.H. and MacGregor, J.G. (1997), "Modification of the ACI rectangular stress block for high-strength concrete", *ACI Structural Journal*, **94**(1), 40-48.
Inel, M., Ozmen, H.B. and Bilgin, H. (2008), "Seismic performance evaluation of school buildings in Turkey", *Structural Engineering and Mechanics*, **30**(5), 535-558.
Lam, S.S.E., Wu, B., Wong, Y.L., Wang, Z.Y., Liu, Z.Q. and Li, C.S. (2003), "Drift capacity of rectangular reinforced concrete columns with low lateral confinement and high-axial load", *Journal of Structural Engineering, ASCE*, **129**(6), 733-742.
Lam, S.S.E., Wu, B., Liu, Z.Q. and Wong, Y.L. (2008), "Experimental study on seismic performance of coupling beams not designed for ductility", *Structural Engineering and Mechanics*, **28**(3), 317-333.
Marefat, M.S., Khanmohammadi, M., Bahrani, M.K. and Goli, A. (2006), "Experimental assessment of reinforced concrete columns with deficient seismic details under cyclic load", *Advances in Structural Engineering*, **9**(3), 337-347.
Mattock, A.H., Kriz, L.B. and Hognestad, E. (1961), "Rectangular concrete stress distribution in ultimate strength design", *ACI Journal*, **57**(1), 875-928.
Mo, Y.L. and Wang, S.J. (2000), "Seismic behavior of RC columns with various tie configurations", *Journal of Structural Engineering, ASCE*, **126**(10), 1122-1130.
Ozbakkaloglu, T. and Saatcioglu, M. (2004), "Rectangular stress block for high-strength concrete", *ACI Structural Journal*, **101**(4), 475-483.
Pam, H.J. and Ho, J.C.M. (2001), "Flexural strength enhancement of confined reinforced concrete columns", *Proceedings of the Institution of Civil Engineers, Structures and Buildings*, **146**(4), 363-370.
Pam, H.J., Kwan, A.K.H. and Islam, M.S. (2001a), "Flexural strength and ductility of reinforced normal- and high-strength concrete beams", *Proceedings, Institution of Civil Engineers, Structures and Buildings*, **146**(4), 381-389.
Pam, H.J., Kwan, A.K.H. and Ho, J.C.M. (2001b), "Post-peak behavior and flexural ductility of doubly reinforced normal- and high-strength concrete beams", *Structural Engineering and Mechanics*, **12**(5), 459-474.
Pam, H.J. and Ho, J.C.M. (2009), "Length of critical region for confinement steel in limited ductility high-strength reinforced concrete columns", *Engineering Structures*, **31**, 2896-2908.
Park, R. (2001), "Improving the resistance of structures to earthquakes", *Bulletin of the New Zealand National Society of Earthquake Engineering*, **34**(1), 1-39.

Pecce, M. and Fabbrocino, G. (1999), "Plastic rotation capacity of beams in normal and high-performance concrete", *ACI Structural Journal*, **96**(2), 290-296.
Peng, J., Ho, J.C.M., Pam, H.J. and Wong, Y.L. (2012), "Equivalent stress block for normal-strength concrete incorporating strain gradient effect", *Magazine of Concrete Research*, **64**(1), 1-20.
Sadjadi, R. and Kianoush, M.R. (2010), "Application of fiber element in the assessment of the cyclic loading behavior of RC columns", *Structural Engineering and Mechanics*, **34**(3), 301-317.
Sheikh, S.A. and Yeh, C.C. (1990), "Tied concrete columns under axial load and flexure", *Journal of Structural Division, ASCE*, **116**(10), 2780-2801.
Standard Australia (2001), *Australian Standard for Concrete Structures AS 3600-2001*, Australia.
Standards New Zealand, NZS 3101 (2006), *Concrete Structures Standard, Part 1 - The Design of Concrete Structures*, Concrete Standard New Zealand, Wellington, New Zealand.
Su, R.K.L., Lam, W.Y. and Pam, H.J. (2009) "Experimental study of plate-reinforced composite deep coupling beams", *The Structural Design of Tall and Special Buildings*, **18**, 235-257.
Tan, T.H. and Nguyen, N.B. (2004), "Determination of stress-strain curves of concrete from flexure tests", *Magazine of Concrete Research*, **56**(4), 243-250.
Tan, T.H. and Nguyen, N.B. (2005), "Flexural behavior of confined high-strength concrete columns", *ACI Structural Journal*, **102**(2), 198-205.
Weerheijm, J., Mediavilla, J. and van Doormaal, J.C.A.M. (2009), "Explosive loading of multi storey RC buildings: Dynamic response and progressive collapse", *Structural Engineering and Mechanics*, **32**(2), 193-212.
Wu, Y.F., Oehlers, D.J. and Griffith, M.C. (2004), "Rational definition of the flexural deformation capacity of RC column sections", *Engineering Structures*, **26**, 641-650.
Yan, Z.H. and Au, F.T.K. (2010) "Nonlinear dynamic analysis of frames with plastic hinges at arbitrary locations", *The Structural Design of Tall and Special Buildings*, **19**(7), 778-801.
Yagob, O., Galal, K. and Naumoski, N. (2009), "Progressive collapse of reinforced concrete structures", *Structural Engineering and Mechanics*, **32**(6), 771-786.
Zhu, Y. and Su, R.K.L. (2010), "Seismic behavior of strengthened reinforced concrete coupling beams by bolted steel plates, Part 2: Evaluation of theoretical strength", *Structural Engineering and Mechanics*, **34**(5), 563-580.

Notations

A_g	Area of column cross-section
A_s	Area of steel bar of tested column
A_{st}	Area of tension steel bar of beam
A_c	Area of concrete compression zone
b	Width of cross section
c	Neutral axis depth
d	Distance of longitudinal steel bar to extreme compressive fibre or effective depth of cross section in Eqs. (3), (4) and (6).
d	Effective depth of column section
d'	The distance from the extreme compressive fibre to the centroid of compression steel
E_s	Young's modulus of steel bar
f_{av}	Average concrete compressive stress over compression area in flexural members
f_{co}	The concrete stress developed in flexure, taken as $\alpha f_c'$
f_c'	Uni-axial concrete compressive strength represented by cylinder strength
f_{cu}	Uni-axial concrete compressive strength represented by cube strength

f_{max} Maximum concrete compressive stress developed under flexure
f_s Stress of steel bar
f_{sc} Stress of compression steel bar
f_{st} Stress of tension steel bar
f_y Yield strength of steel bar
h Height of cross section
k_1 Ratio of average stress (f_{av}) over compression area to maximum stress developed under flexure (f_{max})
k_2 Ratio of distance between extreme compressive fibre and resultant force of compressive stress block (P_c) to that between the same fibre to neutral axis (c)
k_3 Ratio of f_{max} to uni-axial concrete strength f_c' or f_{cu}
LVDT Linear variable displacement transducer
M Moment or flexural strength
M_{ACI} Moment calculated based on ACI code
M_e The experimentally obtained moment of column cross section
M_{EC} Moment calculated based on Eurocode 2
M_{NZ} Moment calculated based on New Zealand Code
M_p Moment calculated based on the proposed values of equivalent rectangular concrete stress block parameters obtained in this study
M_t Measured moment capacity
n Number of longitudinal steel bars
P Axial load
P_e The experimentally obtained axial force of column cross section
PC Plain concrete
P_c Resultant force of concrete compressive stress block
RC Reinforced concrete
α Ratio of equivalent concrete compressive stress developed under flexure to concrete cylinder (f_c') or cube (f_{cu}) strength
β Ratio between height of equivalent rectangular concrete compressive stress block and neutral axis depth
ε Concrete strain
ε_{cu} Ultimate concrete strain at extreme compressive fibre measured at maximum load of eccentrically loaded specimen
ρ_{bo} The balanced steel ratio of beam
ρ_c The compression steel ratio of beam
ρ_s Longitudinal reinforcement ratio of tested column
ρ_t The tension steel ratio of beam
σ Concrete stress
σ_c Concrete compressive stress in concentrically loaded specimen
$\sigma_c(\varepsilon)$ Function of the concrete stress-strain curve obtained from the concentrically loaded specimens
ϕ Strain gradient